RESEARCH PAPER

Reversal of albuminuria by combined AM6545 and perindopril therapy in experimental diabetic nephropathy

Correspondence Dr Federica Barutta, Diabetic Nephropathy Laboratory, Department of Medical Sciences, University of Turin, C/so Dogliotti 14, Turin 10126, Italy. E-mail: federica.barutta@unito.it

F Barutta[1] (iD), S Bellini[1] (iD), R Mastrocola[2] (iD), R Gambino[1] (iD), F Piscitelli[4] (iD), V di Marzo[4] (iD), B Corbetta[1] (iD), VK Vemuri[3] (iD), A Makriyannis[3] (iD), L Annaratone[1] (iD), G Bruno[1] (iD) and G Gruden[1] (iD)

[1]Department of Medical Sciences, University of Turin, Turin, Italy, [2]Department of Clinical and Biological Sciences, University of Turin, Turin, Italy, [3]Center for Drug Discovery, Northeastern University, Boston, MA, USA, and [4]Endocannabinoid Research Group, Institute of Biomolecular Chemistry – CNR, Pozzuoli, Italy

BACKGROUND AND PURPOSE

The endocannabinoid (EC) system has been implicated in the pathogenesis of diabetic nephropathy (DN). We investigated the effects of peripheral blockade of the cannabinoid CB_1 receptor as an add-on treatment to ACE-inhibition in type 1 diabetic mice (DM) with established albuminuria.

EXPERIMENTAL APPROACH

Renal functional parameters (albumin excretion rate, creatinine clearance), tubular injury, renal structure, both EC and CB receptor levels and markers of podocyte dysfunction, fibrosis and inflammation were studied in streptozotocin-induced DM treated for 14 weeks with vehicle, the ACE-inhibitor perindopril (2 mg·kg^{-1}·day^{-1}), peripherally-restricted CB_1 receptor antagonist AM6545 (10 mg·kg^{-1}·day^{-1}) or both. Treatments began at 8 weeks after diabetes onset, when early DN is established.

KEY RESULTS

CB_1 receptors were overexpressed in DM and neither perindopril nor AM6545 altered this effect, while both drugs abolished diabetes-induced overexpression of angiotensin AT_1 receptors. Single treatment with either AM6545 or perindopril significantly reduced progression of albuminuria, down-regulation of nephrin and podocin, inflammation and expression of markers of fibrosis. However, reversal of albuminuria was only observed in mice administered both treatments. The ability of the combination therapy to completely abolish slit diaphragm protein loss, monocyte infiltration, overexpression of inflammatory markers and favour macrophage polarization towards an M2 phenotype may explain this greater efficacy. *In vitro* experiments confirmed that CB_1 receptor activation directly inhibits retinoic acid-induced nephrin expression in podocytes and IL-4-induced M2 polarization in macrophages.

CONCLUSION AND IMPLICATIONS

Peripheral CB_1 receptor blockade used as add-on treatment to ACE-inhibition reverses albuminuria, nephrin loss and inflammation in DM.

Abbreviations

2-AG, 2-arachidonoylglycerol; ACE-I, ACE inhibitors; AEA, anandamide; DM, Diabetic; DN, diabetic nephropathy; EC, endocannabinoid; ECS, endocannabinoid system; MCP-1, monocyte chemoattractant protein-1; RAS, renin angiotensin system; STZ, streptozotocin

Introduction

Diabetic nephropathy (DN) is the leading cause of end-stage renal failure in the Western World and increases the risk of cardiovascular morbidity and mortality in subjects with diabetes (IDF Diabetes Atlas, 2017). Both glycaemic control and inhibition of the renin angiotensin system (RAS) with either ACE inhibitors (ACE-I) or **angiotensin II type 1 (AT$_1$) receptor** blockers are established treatments for diabetic kidney disease (Fineberg et al., 2013). Despite proven efficacy of these therapies, they are insufficient to completely arrest the progression of the disease and there is, thus, the need to identify additional therapeutic tools.

DN is characterized by increased glomerular permeability to proteins and the accumulation of extracellular matrix components in the mesangium, resulting in albuminuria and a progressive decline in renal function (Forbes and Cooper, 2013; Tuttle et al., 2014). Podocytes are components of the glomerular filtration barrier and the slit diaphragm, a junction connecting neighbouring podocytes, is considered the major restriction site to protein filtration. Loss of slit diaphragm proteins, such as nephrin and podocin, plays a key role in the pathogenesis of albuminuria in diabetes (Huh et al., 2002; Nagata, 2016). In addition, low-grade inflammation occurs in the diabetic glomeruli and is believed to amplify the glomerular injury (Barutta et al., 2015; Wada and Makino, 2016).

Recent studies in experimental diabetes have demonstrated that a full endocannabinoid system (ECS) is present in the kidney and that, beyond worsening metabolism, a malfunction of the ECS plays a direct role in the pathogenesis of DN (Janiak et al., 2007; Barutta et al., 2010, 2011, 2014; Russell et al., 2010; Tam et al., 2010; Lim et al., 2011; Nam et al., 2012; Jourdan et al., 2014; Lecru et al., 2015; Gruden et al., 2016; Zoja et al., 2016). The ECS comprises two endogenous cannabinoids, **anandamide (AEA)** and **2-arachidonoylglycerol (2-AG)**, the enzymes that regulate their production and degradation, and two GPCRs, cannabinoid type 1 (**CB$_1$**) and **CB$_2$** receptors, through which they signal. In both animals and humans with diabetes, CB$_1$ receptors are overexpressed in the diabetic glomeruli, predominantly by podocytes (Barutta et al., 2010; Jourdan et al., 2014; Lecru et al., 2015). Enhanced CB$_1$ receptor signalling has both prosclerotic and inflammatory effects, and studies in various animal models of diabetes have demonstrated that both genetic and pharmacological deletion of the CB$_1$ receptor can ameliorate proteinuria and glomerulosclerosis (Janiak et al., 2007; Barutta et al., 2010; Nam et al., 2012; Jourdan et al., 2014).

Although the use of pharmacological compounds that induce global CB$_1$ receptor blockade is not a viable therapeutic option in humans because of their unwanted central side effects, peripherally-restricted CB$_1$ receptor antagonists, which poorly cross the blood–brain barrier, have recently been developed. These compounds are devoid of psychoactive effects, but they appear to retain the beneficial effects of peripheral CB$_1$ receptor antagonism. Indeed, two peripherally-restricted CB$_1$ receptor blockers, **AM6545** and JD5037, have recently been shown to ameliorate DN in animals, raising the hope that CB$_1$ receptor antagonism may represent a potential new tool for the treatment of DN (Jourdan et al., 2014; Barutta et al., 2017).

Multiple levels of interaction between the ECS and RAS have been reported in various cell types. Angiotensin II (Ang-II) can induce both CB$_1$ receptor expression and the release of EC. Moreover, heterodimers can form between the AT$_1$ and CB$_1$ receptor (Rozenfeld et al., 2011; Jourdan et al., 2014). Whether the combination of peripheral CB$_1$ receptor blockade and RAS inhibition would result in additional benefit in DN is as yet unclear, and this is a highly relevant question in view of potential future studies of CB$_1$ receptor antagonists in humans.

Therefore, in the present study we investigated the effects of the peripherally-restricted CB$_1$ receptor antagonist AM6545 as an add-on treatment to the ACE-I **perindopril** in type 1 diabetic mice (DM) with established albuminuria to assess if the combined treatment has an enhanced efficacy.

Methods

Animals and induction of diabetes

Male C57BL6/J mice from Jackson Laboratories (Bar Harbor, ME, USA) were maintained on a normal diet under standard animal housing conditions. Both housing and care of laboratory animals were in accordance with Italian law (D.L.116/1992), and the study was approved by the Ethical Committee of the University of Turin. Diabetes was induced in mice, aged 8 weeks, by an i.p. injection of streptozotocin (STZ) dissolved in citrate buffer pH 4.5 (55 mg·kg^{-1} body wt·day^{-1}) and delivered in five consecutive daily doses on sedated animals. Mice sham-injected with sodium citrate buffer were used as controls. Diabetes onset was confirmed by blood glucose levels >2.50 mg·mL^{-1} 4 weeks after the first dose of STZ (success rate 95%).

Experimental protocol

Treatments began at 8 weeks after diabetes onset, when early DN is established, and continued for 14 weeks. Diabetic (DM) animals were allocated to treatment with vehicle, perindopril, AM6545 or both (six mice per group). Control [non-diabetic (ND)] animals were treated with vehicle or perindopril plus AM6545 (six mice per group). Perindopril was dissolved in distilled water and given by gavage at dose of 2 mg·kg^{-1}. AM6545 was administered daily at the dosage of 10 mg·kg^{-1}. Although AM6545 can be given p.o., i.p. administration was employed to ensure that mice were receiving the established drug dose. Doses were chosen on the basis of previous studies that have proven both their efficacy and selectivity in mice (Barutta et al., 2017). All animals underwent both oral gavages and i.p. injections of either vehicles (water – mixture 18:1:1 of saline/emulphor-620/DMSO) or active drugs dissolved in vehicle. After 14 weeks of treatment, mice were anesthetized using flurane and then killed by decapitation. The kidneys were rapidly dissected and weighed. The right kidney was frozen in N$_2$ and stored at −80°C for both mRNA and protein analysis. Half of the left kidney was fixed in 10% PBS-formalin then paraffin-embedded for light microscopy; the remaining tissue was embedded in optimal cutting temperature compound and snap-frozen in N$_2$.

Metabolic and physiological parameters

Systolic BP was assessed by tail-cuff plethysmography (failure rate <5%) in pre-warmed un-anaesthetized animals, which were acclimatized to the procedure for at least five consecutive days prior to measurements. Glucose levels were measured using a glucometer (Accu-chek; Roche Applied Science) on a drop of blood taken from 4 h fasted animals the day prior to them being killed. At the time of death, blood samples were taken *via* a saphenous vein puncture on sedated mice for glycated haemoglobin and serum creatinine measurements by quantitative immunoturbidimetric latex determination (Sentinel Diagnostic, Milan, Italy) and HPLC respectively. Urine was collected over 18 h, with each mouse individually housed in a metabolic cage and provided with food and water *ad libitum*. Urine collections were performed before treatment and at the end of the study. Urinary albumin concentration was measured by a mouse albumin ELISA kit (Bethyl Laboratories, USA). Urinary glucose was measured by the glucose-oxidase method using a CS-400 auto-chemistry analyser. Creatinine clearance was calculated from serum and urine creatinine concentrations, as determined by HPLC according to ADMCC guidelines (Dunn *et al.*, 2004).

Histological analysis

Paraffin-embedded tissue sections were stained using Periodic acid–Schiff (PAS) staining. The mesangial area was analysed (percentage of glomerular area) from digital pictures of 15 glomeruli per kidney per animal using Axiovision 4.7 software. Glomerular collagen was assessed by picrosirius red staining and the % area of staining quantified by a computer-aided image analysis system (Axiovision-software), whereby 15 glomeruli for each section were analysed. Evaluations were performed in a blinded fashion by two investigators.

mRNA analysis

Total RNA was extracted from the renal cortex using the TRIzol reagent (Invitrogen, Milan, Italy). One microgram of total RNA was reverse transcribed into cDNA using the high-capacity reverse transcription kit from Applied Biosystems (Monza, Italy). Expression of nephrin (Mm00497828), podocin (Mm00499929), **fibronectin** (Mm01256744), **collagen type I** (Mm00483937), CB_1 receptors (Mm01212171), CB_2 receptors (Mm00438286), **ICAM-1** (Mm00516023), **monocyte chemoattractant protein-1 (MCP-1)** (Mm00441242), **CCR2** (Mm00438270), **TNF-α** (Mm00443258), **arginase-1** (Mm00475988), AT_1 receptors (Mm00616371), CD68 (Mm03047340), **CCL3** (Mm00441258), CD206 (Mm01329362), **NOS2** (Mm00440502) and CD163 (Mm00474091) was measured by real-time PCR using pre-developed TaqMan reagents (Applied Biosystems, Monza, Italy). Raw Ct values were calculated using the SDS software and standardized to the expression of hypoxanthine-guanine phosphoribosyltransferase. Relative expression was calculated using the comparative Ct method ($2^{-\Delta\Delta Ct}$). Because housekeeping genes ubiquitously expressed in the renal cortex do not control for variations in the glomerular number per specimen or changes in podocyte number, WT-1, a podocyte-specific gene, was used as endogenous reference for the evaluation of nephrin and podocin expression.

Immunofluorescence

Sections were fixed in cold acetone for 5 min and blocked in 3% BSA. Subsequently, sections were incubated for an hour with primary antibodies directed against Anti-Nephrin (AB_1542487), Anti-Podocin (AB_261982) and Anti-Fibronectin (AB_476976). Following washing, FITC-conjugated donkey anti-guinea pig (Santa Cruz, Glostrup, Denmark) and swine-anti rabbit (DAKO, Glostrup, Denmark) secondary antibodies were added. Sections were examined using an Olympus epifluorescence microscope (Olympus Bx4I), digitized with a high-resolution camera (Carl Zeiss, Oberkochen, Germany) and quantitated using image analysis software (Axiovision 4.7, Zeiss). Results were calculated as percentage positively stained tissue within the glomerular tuft. On average, 20 randomly selected hilar glomerular tuft cross sections were assessed per mouse.

Double immunofluorescence

After being blocked in avidin–biotin, sections were incubated overnight with an anti-CB_1 receptor antibody, followed by incubation with a biotinylated swine anti-rabbit IgG antibody (DAKO, Glostrup, Denmark) and fluorescein isothiocyanate-conjugated streptavidin (Invitrogen, Milan, Italy). Sections were then exposed to an anti-**MAC-2** antibody for 1 h, followed by incubation with Alexa 555-conjugated donkey anti-rat antibody (Invitrogen, Milan, Italy).

Immunohistochemistry

Staining for F4/80 was performed on frozen sections. CB_1 and CB_2 receptor, MAC-2 and p57 expression was detected on 4 μm paraffin sections of formalin-fixed tissue. After antigen retrieval in citrate buffer or fixation in acetone for 10 min, sections were exposed to H_2O_2 to eliminate endogenous peroxidase activity and blocked with avidin-biotin and BSA. The kidney sections were then incubated overnight at 4°C with primary antibodies against Anti-CB_1-receptors (AB_10098690), Anti-CB_2-receptors (AB_10079370), Anti-MAC2 (AB_10060357), Anti-P57 (AB_2078155) and Anti-F4/80 (AB_2098196). The sections were washed with PBS and exposed to secondary antibody, HRP-labelled donkey anti-rat IgG (Jackson ImmunoResearch Laboratories, West Grove, USA) or HRP-labelled swine anti-rabbit IgG (DAKO, Glostrup, Denmark) for 1 h, followed by streptavidin–HRP for 1 h. Diaminobenzidine was used as a chromogen. Results are expressed either as the number of positive cells or as percentage area of positive staining per glomerulus. Evaluations were performed by two investigators in a blinded fashion.

Immunoblotting

Renal cortex specimens were lysed in RIPA buffer, containing 0.5% NP40 (vv^{-1}), 0.5% sodium deoxycholate (wv^{-1}), 0.1% SDS (wv^{-1}), 10 mmol·L^{-1} EDTA and proteases inhibitors. Protein extracts were obtained by centrifugation at $14\,000 \times g$ for 20 min at 4°C, preceded by a 45 min incubation period on ice. Total protein concentration was determined using the DC Protein Assay Kit (Bio-Rad, Milan, Italy). Proteins were separated by SDS-PAGE and electrotransferred to nitrocellulose membrane. Following blocking in 5% non-fat milk in TBS (pH 7.6), membranes were incubated overnight with primary antibodies directed against nephrin, podocin and Anti-AT_1-receptors

(AB_2305402) overnight at 4°C. After being washed, secondary HRP-linked antibodies (Santa Cruz) were added for 1 h. Detection was performed using either the ECL chemiluminescence substrate (GE Healthcare, Milan, Italy) or SuperSignal west pico (Euroclone, Milan, Italy) and visualized on a Gel-Doc system (Bio-Rad). Band intensities were quantified by densitometry. Tubulin was used as internal control.

ELISA

Levels of TNF-α, ICAM-1 and MCP-1 were measured in renal tissue homogenates by commercially available ELISA following the manufacturer's instructions: mouse TNF-α ELISA kit (MyBiosource, San Diego, CA, USA), mouse MCP-1/CCL2 ELISA kit (R&D System, Oxon, UK) and mouse ICAM-1/CD54 Quantikine ELISA kit (R&D System). Levels of cytokines in renal tissue were normalized to total protein concentrations.

Podocyte apoptosis

Apoptosis was assessed by the TUNEL method using the ApopTag *In Situ* Apoptosis Detection Kit (Millipore, Billerica, MA). Results are expressed as the number of positive cells per glomerulus counted in at least 20 randomly selected glomeruli. Slides pretreated with 20 000 units·mL^{-1} of DNase were used as a positive control.

Extraction and quantification of endocannabinoids and EC-related molecules

Frozen kidney tissue samples from ND ($n = 5$) and DM treated with either AM6545, ACE-I or both ($n = 4$ per group) were homogenized in chloroform/methanol/Tris–HCl 50 mM pH 7.4 (2:1:1, vv^{-1}) containing 10 pmol of [^{2}H]-8-AEA, [^{2}H]-4-palmitoylethanolamine (PEA) and [^{2}H]-4-oleoylethanolamide (OEA), and 50 pmol of [^{2}H]-5-2AG as internal deuterated standards (Cayman Chemicals, Ann Arbor, MI, USA). The extract was purified by silica gel mini-columns and the eluted fraction analysed by liquid chromatography atmospheric pressure MS (LC-APCI-MS). Analyses were carried out in the selected ion-monitoring mode using m/z values of 356 and 348 (molecular ions +1 for deuterated and undeuterated AEA), 304 and 300 (molecular ions +1 for deuterated and undeuterated PEA), 330 and 326 (molecular ions +1 for deuterated and undeuterated OEA) and 384.35 and 379.35 (molecular ions +1 for deuterated and undeuterated 2-AG). AEA, OEA, PEA and 2-AG concentrations were calculated by isotope dilution and expressed as pmol·mg^{-1} (2-AG, PEA and OEA) or g (AEA) of wet tissue weight. The concentrations of 2-AG were obtained by adding the amounts of the 2-isomer to those of the 1(3)-isomer, which mostly originates from the isomerization of the former during work-up.

In vitro experiments

Podocytes. Conditionally immortalized human podocytes were cultured as previously described (Saleem *et al.*, 2002). After differentiation and serum deprivation for 24 h, podocytes were exposed to retinoic acid (RA 1 μmol·L^{-1}) for 24 h either in the presence or absence of the selective CB$_1$ receptor agonist ACEA (1 μmol·L^{-1}). Appropriate dilutions of DMSO were used as controls.

Raw264.7 macrophage cell line. Cells were cultured in DMEM, supplemented with 10% FBS. After 24 h of serum-starvation, cells were treated with WIN55,212-2/vehicle (1 μmol·L^{-1}) for 18 h either in the presence or in the absence of AM6545 (1 μmol·L^{-1}) or AM630 (1 μmol·L^{-1}), followed by incubation with IL-4 (5 ng·mL^{-1}; Thermo Scientific) for 6 h. At the end of the experimental period, total RNA was extracted and arginase-1 mRNA levels measured by real-time PCR. GAPDH was used as an internal control.

Data presentation and statistical analysis

Data are presented as mean ± SEM, geometric mean (25th–75-th percentile), or fold change over control as appropriate. Results were analysed by ANOVA. Data with a non-parametric distribution [albumin excretion rate (AER), percentages] were log-transformed prior to analyses. The LDS test was used for *post hoc* comparisons. Values for $P < 0.05$ were considered statistically significant.

Materials

All materials were purchased from Sigma-Aldrich (St Louis, USA) unless otherwise stated. Details of the antibodies used in the study are reported in the Supporting Information Table S1.

AM6545 5-(4-[4-cyanobut-1-ynyl]phenyl)-1-(2,4-dichlorophenyl)-4-methyl-N-(1,1-dioxo-thiomorpholino)-1H-pyrazole-3-carboxamide, a selective CB$_1$ receptor antagonist (Cluny *et al.*, 2010), was kindly provided by V.K. Vemuri. The compound was dissolved in DMSO, stored at −20°C and diluted in 18:1:1 ratio of saline/emulphor-620/DMSO immediately prior to use. WIN55,212-2, ACEA and AM630 were purchased from Cayman (Ann Arbor, MI, USA) and dissolved in DMSO.

Nomenclature of targets and ligands

Key protein targets and ligands in this article are hyperlinked to corresponding entries in http://www.guidetopharmacology.org, the common portal for data from the IUPHAR/BPS Guide to PHARMACOLOGY (Harding *et al.*, 2018), and are permanently archived in the Concise Guide to PHARMACOLOGY 2017/18 (Alexander *et al.*, 2017a,b).

Results

Metabolic and physiological parameters

Table 1 shows both metabolic and physiological parameters measured at the end of the treatment period in all animal groups. As expected, blood glucose, glycated haemoglobin and kidney weight/body weight ratio were significantly higher and body weight significantly lower in DM compared to ND mice. Treatment with perindopril, AM6545 or both did not alter these parameters. Changes in body weight over time are reported in the Supporting Information Figure S1. Systolic BP was in the normal range and did not differ between DM and ND mice, although measurements using a non-invasive tail-cuff method can miss small differences in BP. A significant reduction in systolic BP was observed in mice treated

Table 1

Metabolic and physiological parameters after 14 weeks of treatment

	Body weight (g)	BG (mg·dL^{-1})	Glycated Hb (%)	sBP (mmHg)	KW/BW ratio
ND	29.3 ± 0.42	135 ± 3.21	4.1 ± 0.19	113 ± 4.28	6.2 ± 0.26
ND Combo	29.2 ± 1.47	140 ± 9.85	3.6 ± 0.32	92 ± 3.74*	6.2 ± 054
DM	23.5 ± 0.66#	390 ± 7.33#	12.3 ± 0.42#	109 ± 4.54	7.6 ± 0.50*
DM AM6545	22.0 ± 0.79#	396 ± 31.7#	12.7 ± 0.64#	112 ± 7.16	7.9 ± 0.22*
DM ACE-I	21.7 ± 2.16#	397 ± 25.1#	12.9 ± 0.91#	92 ± 6.77*	7.5 ± 0.54*
DM Combo	22.6 ± 1.39#	346 ± 41.7#	12.4 ± 0.95#	94 ± 6.89*	7.5 ± 0.50*

Data are shown as mean ± SEM or geometric mean (25th–75th percentile); ACE-I, treatment with perindopril; AM6545, treatment with AM6545; BG, blood glucose; Combo, treatment with AM6545 plus perindopril; glycated Hb, glycated haemoglobin; KW/BW, kidney weight/body weight; sBP, systolic BP.

*$P < 0.05$ DM versus ND and ND Combo, DM ACE-I and DM Combo versus others.

#$P < 0.001$ DM versus ND.

with perindopril, and this effect was not modified by AM6545.

ECS system and AT$_1$ receptors

In DM, glomerular immunostaining for CB$_1$ receptors was enhanced, while staining for CB$_2$ receptors was unchanged. Consistent with this, diabetes induced a significant increase in glomerular CB$_1$ receptor mRNA levels without changing the CB$_2$ receptor expression (Figure 1A–F), resulting in a threefold increase in glomerular CB$_1$/CB$_2$ receptor mRNA ratio (Table 2). Moreover, measurement of both EC and EC-related molecules by mass-spectrometry showed a diabetes-induced reduction in the levels of 2-AG, the predominant CB$_2$ receptor ligand (Table 2). Overall, these data indicate a predominant CB$_1$ receptor-mediated EC tone in experimental DN.

Neither EC (Table 2) nor CB receptor levels (Figure 1A–F) were changed by any treatment. On the contrary, the rise in AT$_1$ receptor mRNA and protein expression induced by diabetes was suppressed by all treatments (Figure 1G–I), indicating that both RAS and CB$_1$ receptor blockade can abolish local increased responsiveness to Ang-II.

Albuminuria and renal functional parameters

As shown in Table 3, prior to treatment levels of albuminuria were significantly greater in DM compared with ND mice, indicating the development of early DN. Animals allocated to the different treatment groups had comparable urinary albumin levels. At the end of the treatment period, DM showed at least a threefold increase in albuminuria compared to controls. Single treatments with either AM6545 or perindopril reduced albuminuria by 50%. In DM under dual therapy, albuminuria was comparable to that in ND animals, indicating a reversal of early DN. In DM, neither glycosuria nor the rise in N-acetyl-β(D)-glucosaminidase (NAG) activity/creatinine ratio was ameliorated by treatment with AM6545, alone or in combination with therapy, suggesting that AM6545 acted predominantly at the glomerular levels (Table 3). There was only a modest and non-significant decline in renal function in vehicle-treated DM, which did not allow this functional parameter to be used to assess efficacy of treatments on.

Effect of treatments on podocytes

Diabetes induced a significant reduction in both nephrin and podocin immunostaining. In keeping with the results on albuminuria, this decrease in both nephrin and podocin was reduced by a single treatment with either AM6545 or perindopril, but only the combined treatment abolished the reduction seen in DM. These semi-quantitative data were confirmed by measuring both nephrin and podocin expression in total renal cortex by real-time PCR and Western blotting (Figure 2A–I). Podocyte number did not differ among groups as assessed by counting the p57-positive cells (Figure 2J,K). Furthermore, diabetes-induced apoptosis was modest and did not vary significantly in treated and untreated animals (ND: 0.27 ± 0.06; DM: 0.75 ± 0.07; DM-AM6545: 0.83 ± 0.06; DM-ACE-I: 0.79 ± 0.05; DM Combo: 0.79 ± 0.06; P = NS podocyte number/glomerular area). Therefore, drugs were likely to act directly on nephrin/podocin expression rather than indirectly through prevention of podocyte apoptosis/loss.

CB$_1$ receptor and nephrin expression in cultured podocytes

To clarify the mechanism whereby the CB$_1$ receptor affects nephrin, we tested, *in vitro*, the hypothesis that CB$_1$ receptor signalling may interfere with retinoic acid (RA)-induced nephrin expression. As expected, exposure of cultured podocytes to RA induced a twofold increase in nephrin mRNA levels. CB$_1$ receptor activation with ACEA not only prevented the increase in nephrin in response to RA, but even lowered the nephrin expression below control levels (Figure 2L). This suggests that an increased CB$_1$ receptor-mediated EC tone within the diabetic glomeruli may inhibit the RA-receptor pathway controlling the expression of nephrin.

Renal hypertrophy, mesangial expansion and extracellular matrix components

PAS staining revealed a mild mesangial expansion in DM that was reduced to a similar extent by all treatments. DM-induced overexpression of both collagen type 1 and fibronectin mRNA was reduced by all treatments. Although the effect of dual therapy was slightly greater with a rise in fibronectin
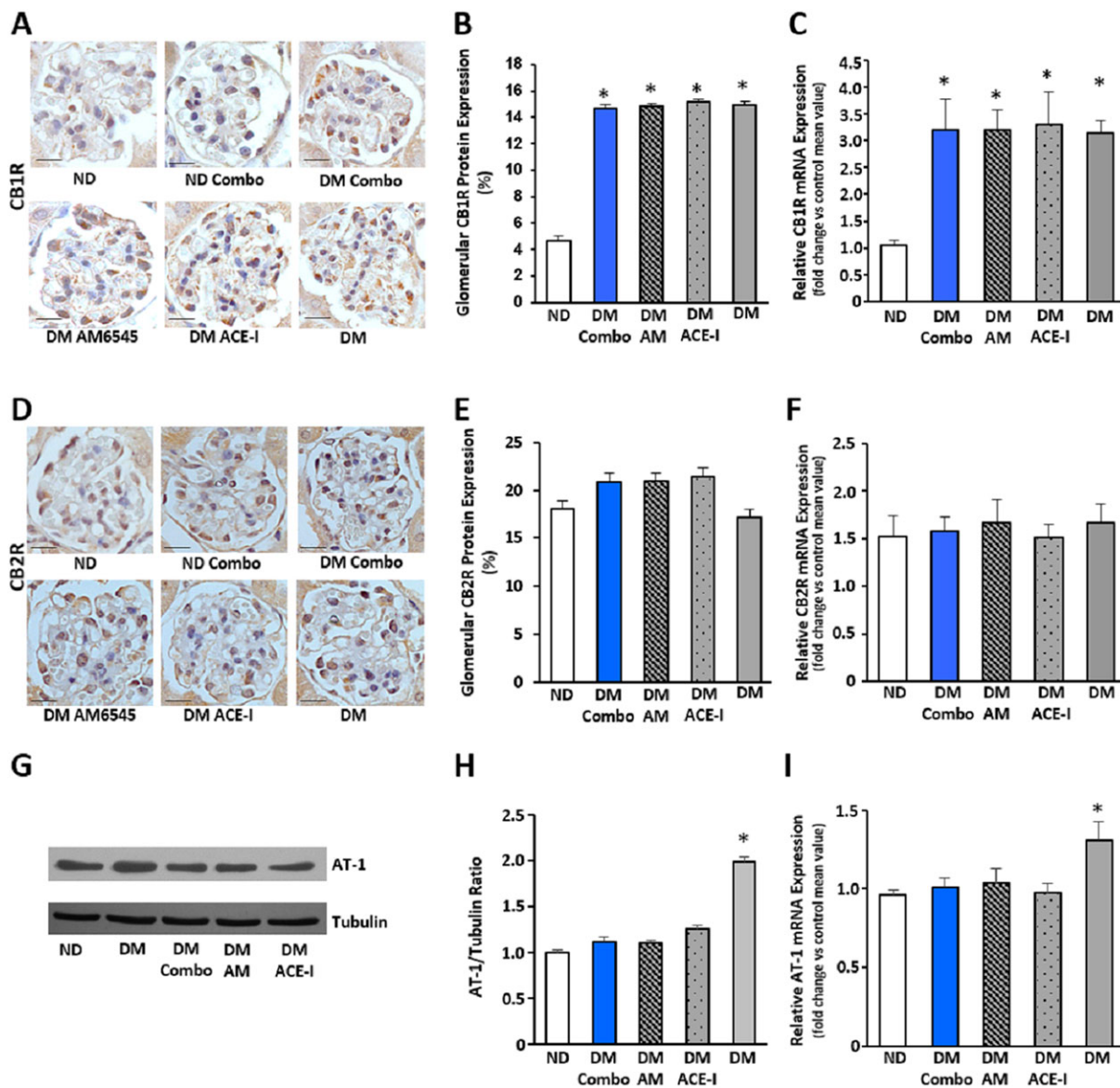
Figure 1

Effect of treatment with AM6545 and/or perindopril on CB_1, CB_2 and AT_1 receptors in DM. Control ND and DM were treated with vehicle, AM6545 (AM), perindopril (ACE-I) or AM6545 plus perindopril (Combo) ($n = 6$ mice per group). Representative immunohistochemistry analysis of CB_1 receptors (A) and CB_2 receptors (D) are shown (original magnification ×400) and quantification of glomerular positive staining reported in the graphs (B–E). CB_1, CB_2 and AT_1 receptor mRNA levels were measured by real-time PCR on total RNA extracted from the renal cortex. Results were corrected for the expression of the housekeeping gene HPRT and shown in the graphs (C, F, I). Representative immunoblot (G) and densitometry analysis (H) of AT_1 receptor protein expression in total protein extracts from the total renal cortex are shown. Tubulin was used as internal control (*$P < 0.05$, vs. ND).

and collagen, which were then no longer significant as compared to controls, the difference between dual and single treatments was modest and not statistically significant. Positive glomerular immunostaining for both fibronectin and collagen was increased by DM and lowered by all treatments, although values returned to control levels only in the combination therapy group (Figure 3).

Monocyte/macrophage accumulation

Immunohistochemical staining revealed that the number of monocytes/macrophages infiltrating the glomeruli, assessed by counting the number of both F4/80 and MAC-2 positive cells, was significantly greater in DM compared to ND mice. The combined therapy abolished DM-induced increase in number of accumulated monocytes/macrophages, while the number of infiltrating monocytes/macrophages fell only by half in mice under single treatments and it was still significantly greater than in control animals (Figure 4A–D). However, the absolute number of monocytes/macrophages was quite low, and thus, results should be treated with caution. A similar trend was observed in the gene expression of the macrophage marker CD68 (Figure 4E) and in both

Table 2

Effect of treatment with AM6545 and/or perindopril on EC/EC-related molecule levels and CB_1/CB_2 receptor mRNA ratio

	2-AG (pmol·mg^{-1})	AEA (pmol·g^{-1})	PEA (pmol·mg^{-1})	OEA (pmol·mg^{-1})	CB_1/CB_2 mRNA ratio
ND	7.05 ± 0.46	2.44 ± 0.21	0.07 ± 0.01	0.21 ± 0.02	0.77 ± 0.14
DM	4.76 ± 0.55*	2.28 ± 0.71	0.09 ± 0.03	0.16 ± 0.02	2.12 ± 0.42*
DM-ACE-I	4.15 ± 1.36*	2.01 ± 0.16	0.10 ± 0.03	0.24 ± 0.05	1.98 ± 0.13*
DM-AM6545	4.61 ± 0.36*	2.81 ± 1.46	0.18 ± 0.07	0.20 ± 0.05	2.14 ± 0.28*
DM-Combo	4.55 ± 0.41*	2.82 ± 0.44	0.12 ± 0.06	0.16 ± 0.03	2.13 ± 0.44*

Data are shown as mean ± SEM; ACE-I, treatment with perindopril; AM6545, treatment with AM6545; Combo, treatment with AM6545 plus perindopril.
*$P < 0.01$ versus ND.

Table 3

Albuminuria and renal functional parameters

	Prior to treatments (8 weeks of diabetes)	At the end of the study (14 weeks of treatments)			
	AER (μg.18 h^{-1})	AER (μg.18 h^{-1})	Cr Cl (mL·min^{-1})	NAG activity (U·g^{-1})	Glycosuria (mg.18 h^{-1})
ND	30.6 (26–36.3)	118.8 (109.5–130.1)	0.47 ± 0.06	65.3 ± 5.47	0.01 ± 0.002
ND Combo	30.9 (25.8–36.1)	111.5 (93.1–127.4)	0.50 ± 0.08	61.2 ± 5.32	0.01 ± 0.005
DM	53.1 (40.4–78.9)*	429.7 (382.8–513.7)*	0.40 ± 0.04	255.7 ± 11.97*	3.83 ± 0.66*
DM AM6545	52.5 (39–83.6)*	242.9 (224.5–275.4)*,†	0.45 ± 0.13	240.6 ± 13.71*	3.18 ± 0.10*
DM ACE-I	53.6 (40.8–79.1)*	235.1 (228.6–260.4)*,†	0.42 ± 0.05	256.7 ± 43.13*	3.15 ± 0.24*
DM Combo	51.3 (34.3–82.7)*	144.8 (132.1–173.4)†,‡	0.48 ± 0.05	249.8 ± 44.24*	3.24 ± 0.37*

Data are shown as mean ± SEM or geometric mean (25th–75th percentile); ACE-I, treatment with perindopril; AM6545, treatment with AM6545; Combo, treatment with AM6545 plus perindopril; Cr Cl, creatinine clearance.
*$P < 0.05$, versus ND.
†$P < 0.05$, versus DM.
‡$P < 0.05$ DM Combo versus single treatments.

mRNA and protein expression of the adhesion molecule ICAM-1 (Figure 4F,G). The combined therapy even reduced ICAM-1 protein levels below control values.

As the chemokine MCP-1 plays a key role in glomerular monocyte accumulation, we also assessed the expression of MCP-1 and its cognate receptor CCR2. DM-induced MCP-1 expression was not altered by single treatments, but it was abolished by dual therapy, and MCP-1 protein levels were significantly lower than in control mice. By contrast, DM-induced CCR2 overexpression was attenuated by all therapies (Figure 4H–J). Therefore, all therapies can normalize responsiveness to MCP-1, but only the combination of both ACE and CB_1 receptor inhibition abolished MCP-1 overexpression, possibly explaining the greater efficacy of dual therapy in lowering the glomerular accumulation of monocytes/macrophages.

M1 and M2 macrophage polarization

Diabetes induced a rise in markers of M1 macrophages (TNF-α, CCL3 and NOS2) that was reduced by single treatments and abolished by dual therapy (Figure 5A–D). Markers of M2 anti-inflammatory macrophages, CD163 and CD206, were down-regulated by diabetes, normalized by single treatments

and significantly increased above control levels by the combined therapy (Figure 5E, F). Moreover, perindopril failed to reverse the DM-induced down-regulation of Arg-1, whereas AM6545, either alone or in combination therapy, not only normalized but also up-regulated Arg-1 mRNA levels (Figure 5G). Because monocyte/macrophages infiltrating the diabetic glomeruli expressed the CB_1 receptor in vivo, they were potential direct targets of AM6545 (Supporting Information Figure S2A).

In vitro M2 polarization

To assess the hypothesis that CB_1 receptor activation can directly affect M2 polarization, we performed in vitro experiments with Raw264.7 macrophages expressing both CB receptors (Supporting Information Figure S2B), and investigated the effect of CB receptor activation on IL-4-induced M2 polarization. The non-selective agonist WIN55,212-2, which activates both CB_1 and CB_2 receptors, markedly reduced the expression of Arg-1 in macrophage exposed to IL-4, indicating that the ECS has an inhibitory effect on M2 macrophage polarization. Moreover, the effect of WIN55,212-2 was abolished by AM6545 and left unchanged
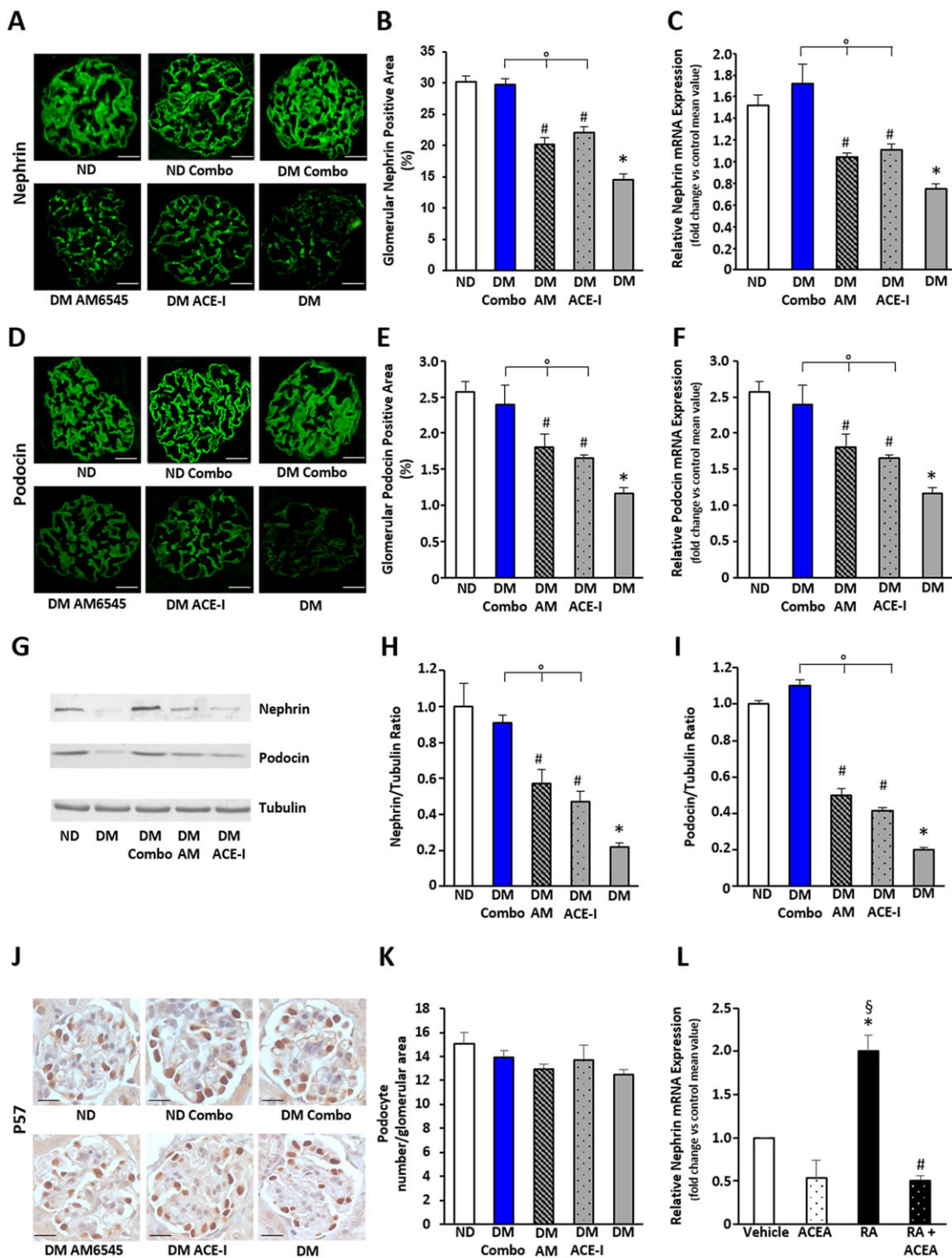
Figure 2

Effect of treatment with AM6545 and/or perindopril on nephrin and podocin expression and podocyte number in DM. Control ND and DM were treated with vehicle, AM6545 (AM), perindopril (ACE-I) or AM6545 plus perindopril (Combo) ($n = 6$ mice per group). Both nephrin (A–C) and podocin (D–F) mRNA and protein expression was assessed. Representative immunofluorescence images of nephrin (A) and podocin (D) are shown (original magnification ×400). Quantification of both glomerular staining (B, E) and mRNA levels (C, F) is reported in the graphs. Representative immunoblots (G) and results of densitometry analysis (H, I) of nephrin and podocin protein expression in total protein extracts from the total renal cortex. Tubulin was used as an internal control. Representative immunohistochemistry images (J original magnification ×400) and quantification of glomerular positive staining of p57 (K) are shown (*$P < 0.05$ vs. ND; #$P < 0.05$ vs. DM; °$P < 0.05$ dual treatment vs. single treatment). (L) Nephrin mRNA levels were measured by real-time PCR on total RNA extracts from podocytes exposed to RA (1 μmol·L^{-1})/vehicle for 24 h in the presence and in the absence of ACEA (1 μmol·L^{-1}) (*$P < 0.05$ RA vs. vehicle; §$P < 0.05$ RA vs. ACEA and RA + ACEA; #$P < 0.05$ RA + ACEA vs. vehicle).
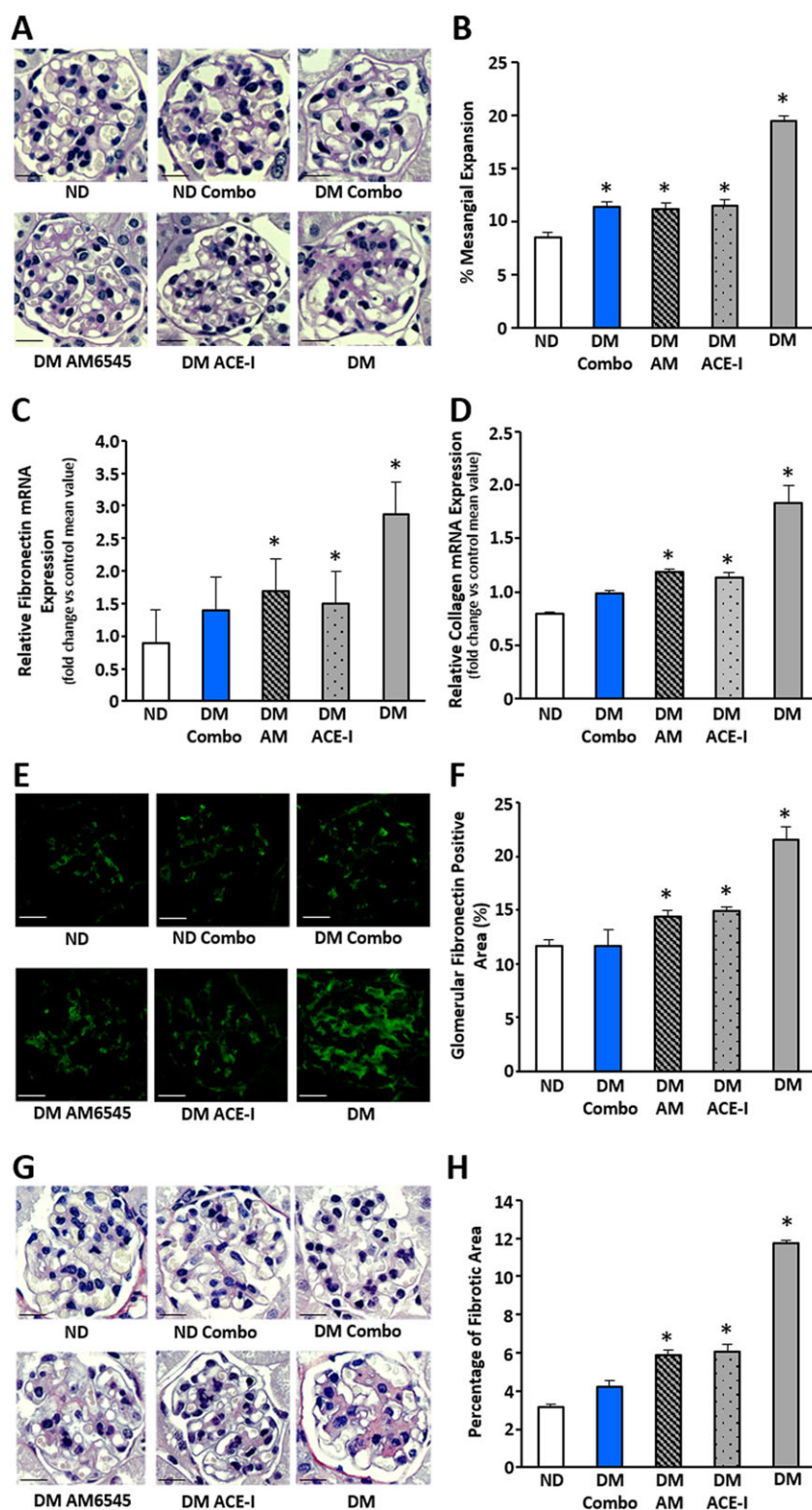
Figure 3
Effect of AM6545 and/or perindopril on markers of fibrosis in DM. ND and DM were treated with vehicle, AM6545 (AM), perindopril (ACE-I) or AM6545 plus perindopril (Combo) (n = 6 mice per group) for 14 weeks. PAS staining was assessed in renal cortex sections. Representative images (scale bar: 50 μm) and percentage PAS glomerular-positive areas are shown (A, B). Both fibronectin (C) and collagen type I (D) mRNA expression was measured by real-time PCR on total RNA extracted from the renal cortex and results are presented in the graphs. Representative images of glomerular fibronectin protein expression (E), picrosirius red staining (G) and quantitation of glomerular staining are shown (F, H) (*P < 0.05 vs. ND).
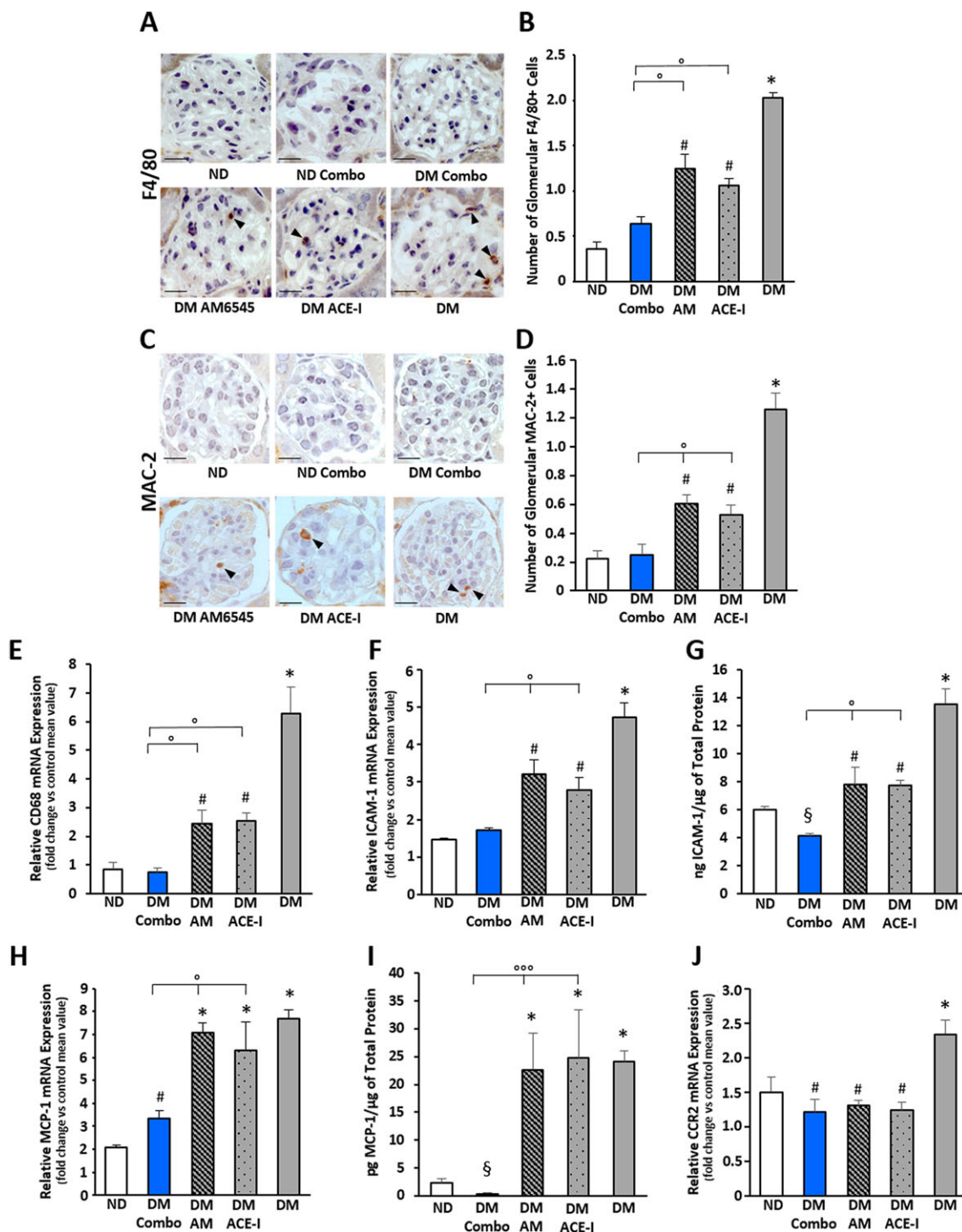
Figure 4

Effect of AM6545 and/or perindopril on diabetes-induced inflammation. ND and DM were treated with vehicle, AM6545 (AM), perindopril (ACE-I) or AM6545 plus perindopril (Combo) (n = 6 mice per group) for 14 weeks. Representative images of glomerular F4/80 (A) and MAC-2 (C) positive immunostaining are shown and quantitation reported in the graph (B, D). Total RNA was extracted from the renal cortex and levels of mRNA encoding for CD68 (E), ICAM-1 (F), MCP-1 (H) and CCR2 (J), measured by real-time PCR. Protein levels of ICAM-1 (G) and MCP-1 (I) in renal tissue were determined by ELISA and normalized to total protein (*$P < 0.05$ vs. ND; #$P < 0.05$ vs. DM group; °$P < 0.05$ dual vs. single treatment; §$P < 0.05$ combo vs. ND).
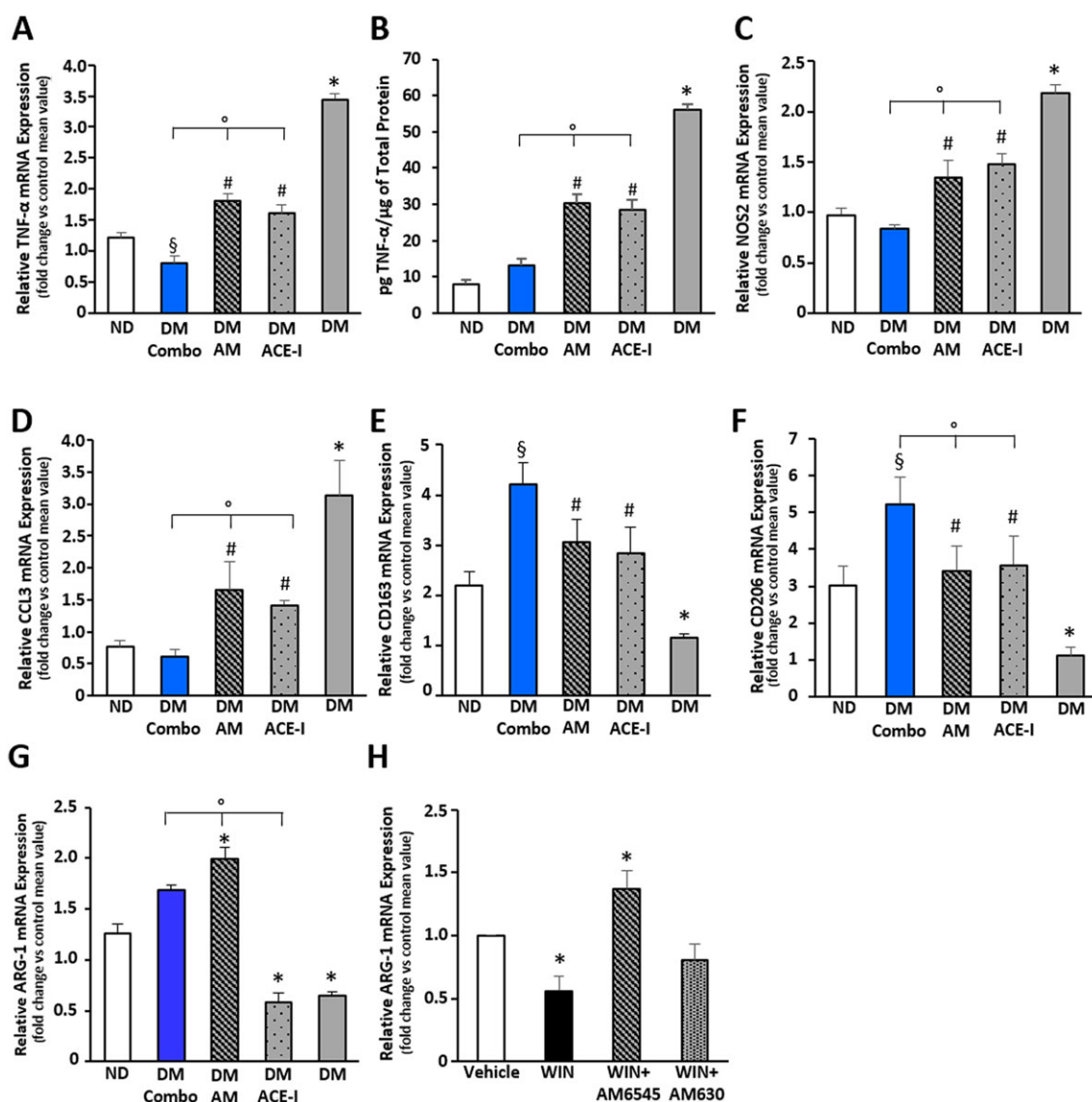
Figure 5
Effect of AM6545 and/or perindopril on macrophage phenotype. ND and DM were treated with vehicle (DM), AM6545 (AM), perindopril (ACE-I) or AM6545 plus perindopril (Combo) ($n = 6$ mice per group) for 14 weeks. Total RNA was extracted from the renal cortex and levels of mRNA encoding for TNF-α (A), NOS2 (C), CCL3 (D), CD163 (E), CD206 (F), arginase-1 (G), measured by real time-PCR. (B) Levels of TNF-α in kidney tissue were determined by ELISA and normalized to total protein (*$P < 0.05$ vs. ND; [#]$P < 0.05$ vs. DM; [°]$P < 0.05$ dual vs. single treatment; [§]$P < 0.05$ combo vs. ND). (H) Arginase-1 mRNA levels were measured by real-time PCR on total RNA extracts from RAW 264.7 cells exposed to WIN55,212-2 (1 μmol·L^{-1})/vehicle for 18 h in the presence and in the absence of AM6545 (1 μmol·L^{-1}) and AM630 (1 μmol·L^{-1}), followed by incubation with IL-4 (5 ng·mL^{-1}) for 6 h (*$P < 0.05$ WIN and AM6545 vs. vehicle).

by the CB$_2$ receptor antagonist AM630, indicating a specific CB$_1$ receptor-mediated effect (Figure 5H).

Discussion

The present study has provided evidence that in an animal model of type 1 diabetes with early DN, peripheral CB$_1$ receptor blockade used as add-on treatment to ACE-inhibition can reverse albuminuria, nephrin loss and reduce inflammation. This is the first study to investigate the renal effect of combined inhibition of CB$_1$ receptors and ACE.

A delayed intervention was chosen to mimic the clinical scenario of introducing therapy in patients with established microalbuminuria. Prior to treatment albuminuria was 1.7-fold higher in DM than in ND mice. Nephropathy progressed over time, and after a further 14 weeks of diabetes, albuminuria was 3.6-fold greater in untreated DM than in controls. Treatment with either AM6545 or perindopril slowed the rate of progression, but albuminuria was still significantly greater than in controls, indicating that delayed treatment is less effective than treatment delivered from the onset of diabetes, reported in previous studies (Trojacanec *et al.*, 2013; Barutta *et al.*, 2017). On the contrary, in mice under dual therapy

albumin excretion rates were similar to control values, proving reversal of increased glomerular permeability to albumin. Renal function was, however, preserved in this animal model, precluding assessment of treatment efficacy on this factor.

Blood glucose and glycated haemoglobin levels were similar in untreated and treated DM, showing dissociation of albuminuria from hyperglycaemia, the former being reversed and the latter remaining unaffected by dual treatment. Although CB_1 receptor blockade has been reported to modestly ameliorate hyperglycaemia in mice with type 1 diabetes by reducing tubular glucose re-adsorption and thus glycosuria (Hinden et al., 2017), this was not observed in our AM6545-treated mice. Treatment with perindopril significantly lowered BP levels, providing evidence of perindopril efficacy, although angiotensin levels were not directly measured. No changes in BP were observed in AM6545-treated mice, and thus, the anti-proteinuric effect of AM6545 appears independent of BP. This is important in the light of recent results showing that systemic CB_1 receptor blockade can improve both BP and metabolic profile in hypertensive and insulin-resistant rats (Schaich et al., 2014). A previous study has reported reversal of albuminuria in obese and hypertensive Zucker Diabetic Fatty (ZDF) rats treated with JD5037 (Jourdan et al., 2014). However, the effect of treatment on BP was not assessed, and the BP-lowering properties of JD5037 in this model may have contributed substantially to efficacy.

The anti-albuminuric effect of dual therapy was likely to be due to the rescue of both nephrin and podocin down-regulation as no changes in podocyte apoptosis/loss were observed. Both AT_1 and CB_1 receptor activation are known to down-regulate nephrin (Jourdan et al., 2014), and the two pathways may overlap as AM6545 abolished AT_1 overexpression consistent with previous findings in experimental type 2 diabetes (Jourdan et al., 2014). However, the greater efficacy of the combined therapy suggests that the mechanisms were partially independent. Both PKC and Akt are involved in Ang-II-mediated nephrin down-regulation. Moreover, Ang-II increases nephrin binding to β-arrestin2, resulting in nephrin endocytosis and loss (Bussolati et al., 2005; Takano et al., 2007; Xiao et al., 2009; Königshausen et al., 2016). The mechanism of CB_1 receptor-induced nephrin down-regulation is less established, but our in vitro data, showing that ACEA prevents RA-induced nephrin expression, suggest that CB_1 receptors may act via inhibition of the cAMP-RA receptor pathway. In keeping with this, CB_1 receptor activation reduced cAMP levels in cultured podocytes, and a similar mechanism of nephrin down-regulation was described in response to TNF-a (Saito et al., 2010; Jourdan et al., 2014). This is also of relevance given the growing evidence of a key role of RA in podocytes for both differentiation and regeneration (Lazzeri et al., 2014).

Changes in renal haemodynamic are unlikely to explain the superior anti-albuminuric effect of the combination therapy as AEA reduces glomerular capillary pressure (GCP) via CB_1 receptors (Koura et al., 2004), and thus, AM6545 may limit the benefit of lowering GCP through ACE-inhibition. The potential role of the tubuli in the reversal of albuminuria cannot be excluded as CB1R has been implicated in tubular cell apoptosis, trans-differentiation in myofibroblasts (Jenkin et al., 2012; Lecru et al., 2015), and reduced albumin reuptake through megalin down-regulation

(Jourdan et al., 2018). However, NAG activity, a marker of tubular injury, was not affected by treatments, and the relevance of the tubuli in diabetic albuminuria remains highly controversial (Jarad and Miner, 2009).

The expression of CB_1 receptors was increased in DM, and this was not altered by any treatments. On the contrary, in a study performed in ZDF rats, CB_1 receptor overexpression was reduced by losartan, supporting a direct link between AT_1 receptor activation and CB_1 receptor expression (Jourdan et al., 2014). The reason of this discrepancy is unknown; however, the different animal model is a possible explanation. Auto-induction of CB_1 receptors has been consistently demonstrated in models of type 2 diabetes at variance with STZ-induced diabetes, suggesting a different mechanism of CB_1 receptor up-regulation (Nam et al., 2012; Jourdan et al., 2014). Moreover, obesity and insulin resistance may partially explain the link between RAS activation and CB_1 receptor expression in ZDF rats as increasing evidence suggests an interaction between the ECS and the RAS mediated by the metabolic syndrome.

It has been proposed that enhanced CB_1 receptor expression/signalling in podocytes may represent a final common pathway whereby both hyperglycaemia/DM and Ang-II cause podocyte dysfunction. Our data showing an additive effect of CB_1 receptor and ACE blockade in reversing both the albuminuria and nephrin down-regulation, together with the lack of effect of perindopril on glomerular CB_1 receptor overexpression and renal EC levels, do not support this hypothesis and, instead, provide a rationale for the use of a combined therapy.

Despite a modest glomerular monocyte/macrophage infiltration, a marked rise in inflammatory cytokines was seen in DM, showing that inflammatory/resident cells can trigger cascades amplifying the inflammatory response. Dual therapy performed better than single treatments on inflammation as it abolished both monocyte infiltration and TNF-α overexpression, and it was the only effective treatment in lowering MCP-1. This is of relevance as the chemokine MCP-1 can also induce extracellular matrix production in mesangial cells and nephrin loss in podocytes and MCP-1 deletion ameliorates both proteinuria and glomerulosclerosis in experimental diabetes (Chow et al., 2006; Giunti et al., 2006, 2008; Tarabra et al., 2009).

There was a shift towards a pro-inflammatory M1 macrophage polarization in DM as demonstrated by the overexpression of M1 and down-regulation of M2 macrophage markers. This was reduced by the monotherapies. Therefore, our data do not confirm that ACE-inhibition may promote a deleterious M1-polarization in experimental DN (Cucak et al. 2015). The effect of the dual therapy was greater, particularly on M2 markers. The expression of both CD163 and CD206 rose above control levels in mice under dual treatment. Moreover, the expression of Arg-1, a key switch in M2-polarization, was reduced by diabetes, left unchanged by perindopril and up-regulated by AM6545, either alone or as a combination therapy. The direct effect of CB_1 receptors on M2 polarization was further confirmed by our experiments on RAW267 macrophages showing that a cannabinoid agonist inhibited IL-4-induced M2 polarization in a CB_1 receptor-dependent manner, while CB_2 receptor blockade was not effective. Moreover, neither CB_2 receptor expression nor 2-AG levels

were altered in AM6545-treated mice, making an indirect CB_2 receptor-mediated effect unlikely. This is also in agreement with our previous data showing that treatment with a CB_2 receptor agonist does not alter Arg-1 expression in the renal cortex of DM (Barutta *et al.,* 2017).

Because enhanced M2 polarization occurred in the presence of a normal number of macrophages, this suggests that dual treatment and in particular AM6545 may affect resident macrophages and induce their re-education towards an M2-phenotype. This is of pathophysiological relevance as M2-macrophages express scavenging receptors and produce various anti-inflammatory mediators that promote the resolution of inflammation and tissue repair (Murray 2017). A beneficial effect of M2-macrophages has been shown in models of acute kidney injury, although their role in chronic kidney diseases is more uncertain (Guiteras *et al.* 2016).

Although a low-grade inflammation is considered important in driving fibrotic processes, glomerular PAS staining was reduced to a similar extent by all treatments. The effect of dual therapy on the expression of ECM was slightly greater than that of single treatments, but differences were modest. Therefore, our data failed to show that dual therapy is superior to standard therapy with an ACE-I in preventing fibrosis. However, studies in animal models more prone to develop glomerulosclerosis are required to specifically address this question.

Our results may be of relevance for DN in humans. The current standard therapy for DN with RAS-blockers is insufficient to completely halt disease progression. The potential benefit of CB_1 receptor antagonists as an add-on therapy was assessed in mice with established albuminuria. Therefore, we used a clinically relevant model, reflecting the current indications for treatment. Our results, showing a superior effect of dual therapy on albuminuria, nephrin loss and inflammation, raise hope that CB_1 receptor blockade may be a valuable therapeutic option as an additional therapy. Although further studies in more advanced DN are required, reversal of albuminuria is by itself clinically relevant as it has been associated with a slower early decline of renal function and better cardiovascular outcomes in clinical studies in humans (Jansson *et al.,* n.d.; Perkins *et al.,* 2007).

Acknowledgement

Author contributions

F.B. wrote the manuscript, performed experiments and analysed data; R.M., R.G., S.B., L.A., F.B. and B.C. performed experiments; K.V., A.M., V.D.M. and G.B. edited the manuscript; G.G. wrote the manuscript.

Conflict of interest

The authors declare no conflicts of interest.

Declaration of transparency and scientific rigour

This Declaration acknowledges that this paper adheres to the principles for transparent reporting and scientific rigour of preclinical research recommended by funding agencies, publishers and other organisations engaged with supporting research.

References

Alexander SPH, Christopoulos A, Davenport AP, Kelly E, Marrion NV, Peters JA *et al*. (2017a). The Concise Guide to PHARMACOLOGY 2017/18: G protein-coupled receptors. Br J Pharmacol 174: S17–S129.

Alexander SPH, Fabbro D, Kelly E, Marrion NV, Peters JA, Faccenda E *et al*. (2017b). The Concise Guide to PHARMACOLOGY 2017/18: Enzymes. Br J Pharmacol 174: S272–S359.

Barutta F, Bruno G, Grimaldi S, Gruden G (2015). Inflammation in diabetic nephropathy: moving toward clinical biomarkers and targets for treatment. Endocrine 48: 730–742.

Barutta F, Corbelli A, Mastrocola R Gambino R, Di Marzo V, Pinach S *et al*. (2010). Cannabinoid receptor 1 blockade ameliorates albuminuria in experimental diabetic nephropathy. Diabetes 59: 1046–1054.

Barutta F, Grimaldi S, Franco I, Bellini S, Gambino R, Pinach S *et al*. (2014). Deficiency of cannabinoid receptor of type 2 worsens renal functional and structural abnormalities in streptozotocin-induced diabetic mice. Kidney Int 86: 979–990.

Barutta F, Grimaldi S, Gambino R, Vemuri K, Makriyannis A, Annaratone L *et al* (2017). Dual therapy targeting the endocannabinoid system prevents experimental diabetic nephropathy. Nephrol Dial Transplant 32: 1655–1665.

Barutta F, Piscitelli F, Pinach S, Bruno G, Gambino R, Rastaldi MP *et al*. (2011). Protective role of cannabinoid receptor type 2 in a mouse model of diabetic nephropathy. Diabetes 60: 2386–2396.

Bussolati B, Deregibus MC, Fonsato V, Doublier S, Spatola T, Procida S *et al*. (2005). Statins prevent oxidized LDL-induced injury of glomerular podocytes by activating the phosphatidylinositol 3-kinase/AKT-signaling pathway. J Am Soc Nephrol 16: 1936–1947.

Chow FY, Nikolic-Paterson DJ, Ozols E, Atkins RC, Rollin BJ, Tesch GH (2006). Monocyte chemoattractant protein-1 promotes the development of diabetic renal injury in streptozotocin-treated mice. Kidney Int 69: 73–80.

Cluny NL, Vemuri VK, Chambers AP, Limebeer CL, Bedard H, Wood JT *et al*. (2010). A novel peripherally restricted cannabinoid receptor antagonist, AM6545, reduces food intake and body weight, but does not cause malaise, in rodents. Br J Pharmacol 161: 629–642.

Cucak H, Nielsen Fink L, Højgaard Pedersen M, Rosendahl A (2015). Enalapril treatment increases T cell number and promotes polarization towards M1-like macrophages locally in diabetic nephropathy. Int Immunopharmacol 25: 30–41.

Dunn SR, Qi Z, Bottinger EP, Breyer MD, Sharma K (2004). Utility of endogenous creatinine clearance as a measure of renal function in mice. Kidney Int 65: 1959–1967.

Fineberg D, Jandeleit-Dahm KA, Cooper ME (2013). Diabetic nephropathy: diagnosis and treatment. Nat Rev Endocrinol 9: 713–723.

Forbes JM, Cooper ME (2013). Mechanisms of diabetic complications. Physiol Rev 93: 137–188.

Giunti S, Pinach S, Arnaldi L, Viberti G, Perin PC, Camussi G et al. (2006). The MCP1/CCR2 system has direct proinflammatory effects in human mesangial cells. Kidney Int 69: 856–863.

Giunti S, Tesch GH, Pinach S, Burt DJ, Cooper ME, Cavallo-Perin P et al. (2008). Monocyte chemoattractant protein-1 has prosclerotic effects both in a mouse model of experimental diabetes and in vitro in human mesangial cells. Diabetologia 51: 198–207.

Gruden G, Barutta F, Kunos G, Pacher P (2016). Role of the endocannabinoid system in diabetes and diabetic complications. Br J Pharmacol 173: 1116–1127.

Guiteras R, Flaquer M, Cruzado JM (2016). Macrophage in chronic kidney disease. Clin Kidney J 9: 765–771.

Harding SD, Sharman JL, Faccenda E, Southan C, Pawson AJ, Ireland S et al. (2018). The IUPHAR/BPS Guide to PHARMACOLOGY in 2018: updates and expansion to encompass the new guide to IMMUNOPHARMACOLOGY. Nucl Acids Res 46: D1091–D1106.

Hinden L, Udi S, Drori A, Gammal A, Nemirovski A, Hadar R et al. (2017). Modulation of renal GLUT2 by the cannabinoid-1 receptor: implications for the treatment of diabetic nephropathy. J Am Soc Nephrol 29: 434–448.

Huh W, Kim DJ, Kim MK, Kim YG, Oh HY, Ruotsalainen V et al. (2002). Expression of nephrin in acquired human glomerular disease. Nephrol Dial Transplant 17: 478–484.

IDF Diabetes Atlas (2017). 7th Edition. Available at http://www.diabetesatlas.org (accessed 13/7/2017).

Janiak P, Poirier B, Bidouard JP, Cadrouvele C, Pierre F, Gouraud L et al. (2007). Blockade of cannabinoid CB1 receptors improves renal function, metabolic profile, and increased survival of obese Zucker rats. Kidney Int 72: 1345–1357.

Jansson F, Forsblom C, Harjutsalol V, Thorn L, Wadén J, Elonen N et al. (2018). Regression of albuminuria and its association with incident cardiovascular outcomesand mortality in type 1 diabetes: the FinnDiane Study. Diabetologia 61: 1203–1211.

Jarad G, Miner JH (2009). Albuminuria, wherefore art thou? J Am Soc Nephrol 20: 455–457.

Jenkin KA, Verty AN, McAinch AJ, Hryciw DH (2012). Endocannabinoids and the renal proximal tubule: an emerging role in diabetic nephropathy. Int J Biochem Cell Biol 44: 2028–2031.

Jourdan T, Szanda G, Rosenberg AZ, Tam J, Earley BJ, Godlewski G et al. (2014). Overactive cannabinoid 1 receptor in podocytes drives type 2 diabetic nephropathy. Proc Natl Acad Sci U S A 111: E5420–E5428.

Jourdan T, Park JK, Varga ZV, Pálóczi J, Coffey NJ, Rosenberg AZ et al. (2018). Cannabinoid-1 receptor deletion in podocytes mitigates both glomerular and tubular dysfunction in a mouse model of diabetic nephropathy. Diabetes Obes Metab 20: 698–708.

Königshausen E, Zierhut UM, Ruetze M, Potthoff SA, Stegbauer J, Woznowski M et al. (2016). Angiotensin II increases glomerular permeability by β-arrestin mediated nephrin endocytosis. Sci Rep 6: 39513.

Koura Y, Ichihara A, Tada Y, Kaneshiro Y, Okada H, Temm CJ et al. (2004). Anandamide decreases glomerular filtration rate through predominant vasodilation of efferent arterioles in rat kidneys. J Am Soc Nephrol 15: 1488–1494.

Lazzeri E, Peired AJ, Lasagni L, Romagnani P (2014). Retinoids and glomerular regeneration. Semin Nephrol 34: 429–436.

Lecru L, Desterke C, Grassin-Delyle S, Chatziantoniou C, Vandermeersch S, Devocelle A et al. (2015). Cannabinoid receptor 1 is a major mediator of renal fibrosis. Kidney Int 88: 72–84.

Lim JC, Lim SK, Park MJ, Kim GY, Han HJ, Park SH (2011). Cannabinoid receptor 1 mediates high glucose-induced apoptosis via endoplasmic reticulum stress in primary cultured rat mesangial cells. Am J Physiol Renal Physiol 301: F179–F188.

Murray PJ (2017). Macrophage polarization. Annu Rev Physiol 10: 541–566.

Nagata M (2016). Podocyte injury and its consequences. Kidney Int 86: 1221–1230.

Nam DH, Lee MH, Kim JE, Song HK, Kang YS, Lee JE et al. (2012). Blockade of cannabinoid receptor 1 improves insulin resistance, lipid metabolism, and diabetic nephropathy in db/db mice. Endocrinology 153: 1387–1396.

Perkins BA, Ficociello LH, Ostrander BE, Silva KH, Weinberg J, Warram JH et al. (2007). Microalbuminuria and the risk for early progressive renal function decline in type 1 diabetes. J Am Soc Nephrol 18: 1353–1361.

Rozenfeld R, Gupta A, Gagnidze K, Lim MP, Gomes I, Lee-Ramos D et al. (2011). AT1R-CB1R heteromerization reveals a new mechanism for the pathogenic properties of angiotensin II. EMBOJ 3: 2350–2363.

Russell JC, Kelly SE, Diane A, Wang Y, Mangat R, Novak S et al. (2010). Rimonabant-mediated changes in intestinal lipid metabolism and improved renal vascular dysfunction in the JCR:LA-cp rat model of prediabetic metabolic syndrome. Am J Physiol Gastrointest Liver Physiol 299: G507–G516.

Saito Y, Okamura M, Nakajima S, Hayakawa K, Huang T, Yao J et al. (2010). Suppression of nephrin expression by TNF-alpha via interfering with the cAMP-retinoic acid receptor pathway. Am J Physiol Renal Physiol 298: F1436–F1444.

Saleem MA, O'Hare MJ, Reiser J, Coward RJ, Inward CD, Farren T et al. (2002). A conditionally immortalized human podocyte cell line demonstrating nephrin and podocin expression. J Am Soc Nephrol 13: 630–638.

Schaich CL, Shaltout HA, Brosnihan KB, Howlett AC, Diz DI (2014). Acute and chronic systemic CB1 cannabinoid receptor blockade improves blood pressure regulation and metabolic profile in hypertensive (mRen2)27 rats. Physiol Rep 2: e12108. https://doi.org/10.14814/phy2.12108.

Takano Y, Yamauchi K, Hayakawa K, Hiramatsu N, Kasai A, Okamura M et al. (2007). Transcriptional suppression of nephrin in podocytes by macrophages: roles of inflammatory cytokines and involvement of the PI3K/Akt pathway. FEBS Lett 581: 421–426.

Tam J, Vemuri VK, Liu J, Bátkai S, Mukhopadhyay B, Godlewski G et al. (2010). Peripheral CB1 cannabinoid receptor blockade improves cardiometabolic risk in mouse models of obesity. J Clin Invest 120: 2953–2966.

Tarabra E, Giunti S, Barutta F, Salvidio G, Burt D, Deferrari G et al. (2009). Effect of the monocyte chemoattractant protein-1/CC chemokine receptor 2 system on nephrin expression in streptozotocin-treated mice and human cultured podocytes. Diabetes 58: 2109–2118.

Trojacanec J, Zafirov D, Labacevski N, Jakjovski K, Zdravkovski P, Trojacanec P et al. (2013). Perindopril treatment in streptozotocin induced diabetic nephropathy. Pril (Makedon Akad Nauk Umet Odd Med Nauki) 34: 99–108.

Tuttle KR, Bakris GL, Bilous RW, Chiang JL, de Boer IH, Goldstein-Fuchs J *et al*. (2014). Diabetic kidney disease: a report from an ADA Consensus Conference. Diabetes Care 37: 2864–2883.

Wada J, Makino H (2016). Innate immunity in diabetes and diabetic nephropathy. Nat Rev Nephrol 12: 13–26.

Xiao H, Shi W, Liu S, Wang W, Zhang B, Zhang Y *et al*. (2009). 1, 25-Dihydroxyvitamin D_3prevents puromycin aminonucleoside-induced apoptosis of glomerular podocytes by activating the phosphatidylinositol 3-kinase/Akt-signaling pathway. Am J Nephrol 30: 34–43.

Zoja C, Locatelli M, Corna D, Villa S, Rottoli D, Nava V *et al*. (2016). Therapy with a selective cannabinoid receptor type 2 agonist limits albuminuria and renal injury in mice with type 2 diabetic nephropathy. Nephron 132: 59–69.

Supporting Information

Additional supporting information may be found online in the Supporting Information section at the end of the article.

https://doi.org/10.1111/bph.14495

Figure S1 Changes in body weight over time in the study groups. Body weight was measured in all animal groups prior to streptozotocin (STZ)/vehicle injection (time: 0), at the start of treatment (time: 8 weeks) and at the end of the study (time: 22 weeks). ND, non-diabetic mice; DM, diabetic mice; ACE-I, treatment with perindopril; AM6545, treatment with AM6545; Combo, treatment with AM6545 plus perindopril (***$P < 0.001$ ND vs. DM).

Figure S2 EC receptor expression by macrophages. (A) Double immunofluorescence for CB1R and MAC-2 performed in renal cortex sections from diabetic mice showed colocalization as shown in the merge image. Nuclei were counterstained with DAPI. The dashed square delimits the area shown at higher magnification in the insert. (B) CB1R and CB2R mRNA expression was assessed by PCR in total RNA extracts from RAW 264.7 cells. A representative 2% agarose gel stained with ethidium bromide is shown MW, molecular weight marker.

Table S1 Antibodies features and concentrations.